EFFICIENT ANTI-ALIASING OF A COMPLEX POLYGONAL OSCILLATOR

Christoph Hohnerlein
Quality & Usability Lab,
Technische Universität Berlin
Berlin, Germany
mail@chohner.com

Maximilian Rest
E-RM Erfindungsbüro
Berlin, Germany
m.rest@e-rm.de

Julian D. Parker
Native Instruments GmbH
Berlin, Germany
julian.parker@
native-instruments.de

ABSTRACT

Digital oscillators with discontinuities in their time domain signal derivative suffer from an increased noise floor due to the unbound spectrum generated by these discontinuities. Common anti-aliasing schemes that aim to suppress the unwanted fold-back of higher frequencies can become computationally expensive, as they often involve repeated sample rate manipulation and filtering.

In this paper, the authors present an effective approach to applying the four-point polyBLAMP method to the continuous order polygonal oscillator by deriving a closed form expression for the derivative jumps which is only valid at the discontinuities. Compared to the traditional oversampling approach, the resulting SNR improvements of 20 dB correspond to 2–4× oversampling at 25× lower computational complexity, all while offering a higher suppression of aliasing artifacts in the audible range.

1. INTRODUCTION

A novel complex oscillator algorithm was recently proposed [1], which generates waveforms by traversing a two-dimensional polygon over time. Such a polygon may contain any number of vertices, corresponding to a desired order $n > 2$, which expresses the vertices per rotation. The term complex conveniently combines both the internal dependence on the complex plane as well as the resulting complex spectral behaviour. A projection of the path around a shape in the complex plane can be interpreted as a time-domain signal, with the rotational speed corresponding to the fundamental pitch. Such a signal will naturally contain a number of discontinuities in its derivative. These discontinuities produce an unbounded spectrum and therefore introduce aliasing artifacts into the signal. In order to produce high-quality audio output, this aliasing should be minimized.

Anti-aliasing of digital oscillator algorithms is a well developed topic in literature, but to-date was focused primarily on the generation of classical waveforms or on wavetable synthesis. Research into the anti-aliasing of classical analog waveforms began with the invention of the Band Limited Impulse Train (BLIT) method [2], which generates all waveforms by integrating an underlying sequence of bandlimited impulses. The next major advancement was the invention of the Band Limited stEP (BLEP), and derived Band Limited rAMP (BLAMP) methods [3], which can be applied to the anti-aliasing of discontinuities (of any order) in any type of waveform, as long as the position and magnitude of the discontinuity is known. Further research has concentrated on more efficient polynomial approximations of the ideal BLEP, known as polyBLEP [4, 5, 6, 7].

A parallel stream of research has investigated techniques based on pre-integration of the waveform to be generated, followed by digital differentiation. These techniques have been applied to classical waveforms [8, 9] and to wavetable synthesis [10, 11]. Work has also explored techniques that are a hybrid of these two streams [12, 13]. More recently, both approaches to anti-aliasing have been generalized to apply to the processing of arbitrary input signals with a nonlinear waveshaping function [14, 15, 16, 17, 18].

In the following Section 2, the implementation of the polygon-based oscillator is layed out, which is then anti-aliased in Section 3. The results in terms of SNR and performance are discussed in Section 4, followed by a short summary in Section 5.

2. POLYGON OSCILLATOR

The following is a quick recap of the continuous order polygon waveform synthesis presented in [1]. To create the polygon P of order n, where n denotes the number of vertices after one rotation of the sampling phasor, a corresponding radial amplitude $p(\varphi)$ is generated:

$$p(\varphi) = \frac{\cos\left(\frac{\pi}{n}\right)}{\cos\left[\frac{2\pi}{n} \cdot \mathrm{mod}\left(\frac{\varphi n}{2\pi}, 1\right) - \frac{\pi}{n}\right]} , \tag{1}$$

where φ is a linearly incrementing phase whose slope depends on the desired pitch f_0. The amplitude $p(\varphi)$ can then used to scale a unit circle, resulting in the polygon P in the complex plane:

$$P(\varphi) = p(\varphi) \cdot e^{j\varphi} \tag{2}$$

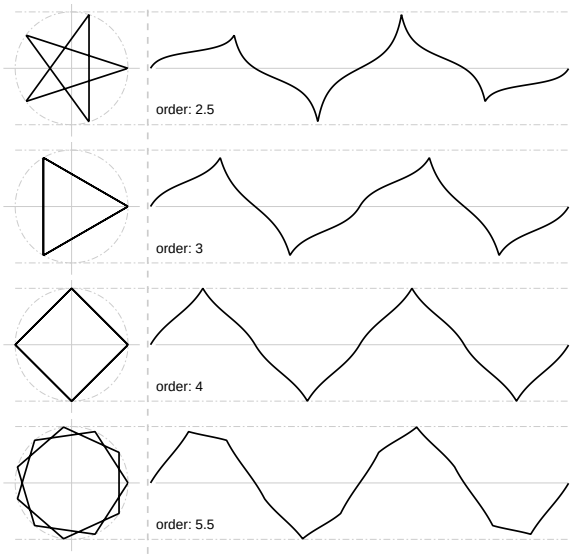

Figure 1: Projections of polygons $P(\phi)$ of different orders n from the 2D space (left) radially sampled into the time domain (right).

Real and imaginary projections x, y then form a 90° phase shifted quadrature output which can be interpreted as oscillator signals in the time domain:

$$f_x(\varphi) = \quad \Re\{\, P(\varphi)\,\} = \cos(\varphi)\cdot p(\varphi) \tag{3}$$
$$f_y(\varphi) = \quad \Im\{\, P(\varphi)\,\} = \sin(\varphi)\cdot p(\varphi) \tag{4}$$

Several of such polygons $P(\varphi, n)$ and their corresponding time-domain projections $f_x(\varphi)$ are shown in Figure 1. One can see that with increasing order / edge count n, the polygon naturally approaches a unit circle, which corresponds to a pure sine in the time domain when sampled spatially. A more in-depth analysis of the link between the shape of the polygon and the resulting spectrum can be found in [1].

3. ANTI-ALIASING

Anti-aliasing of the polygon oscillator could be achieved via most of the available approaches. However, the BLAMP technique is particularly suited to this problem, as the exact positioning and magnitude of the discontinuities in the derivative of the waveform can be obtained in a very efficient closed-form solution.

To apply a four-point polyBLAMP based on third-order B-spline approximation (as presented in [18]), the jump of the first order derivative has to be evaluated at the points of discontinuities, along with the the fractional delay d between the exact time of the discontinuity and the next sample in discrete, sampled time. Table 1 lists the corresponding polynomials that are to be subtracted from the four samples surrounding the discontinuity.

$[-2T, -T]$	$d^5/120$
$[-T, 0]$	$[-3d^5 + 5d^4 + 10d^3 + 10d^2 + 5d + 1]/120$
$[0, T]$	$[3d^5 - 10d^4 + 40d^2 - 60d + 28]/120$
$[T, 2T]$	$[-d^5 + 5d^4 - 10d^3 + 10d^2 - 5d + 1]/120$

Table 1: Four-point polyBLAMP residual for the four samples surrounding a discontinuity, where d is the fractional delay.

3.1. Fractional delay

In the sampled digital time domain, the samples left and right of the discontinuity can be traced from the continuous form, as the positions of the discontinuities are exactly at $\varphi = 2\pi/n \cdot k, k \in [0, 1, ..., \infty)$. The fractional delays d are the difference between the ceiled sample time and the exact time:

$$d = \lceil f_s/(nf_0)\cdot k\rceil - f_s/(nf_0)\cdot k\ , \tag{5}$$

where $\lceil\cdot\rceil$ denotes the ceiling function, f_0 is the fundamental pitch and f_s is the sampling frequency.

Figure 2 shows the discrete time-domain signal $f(\varphi)$ along with its derivative $f'(\varphi)$ while marking the precise positions and amplitude jumps of the derivative at the discontinuities as x and their quantized position by ○.

3.2. Derivative jump at discontinuity

To properly scale the residuum of table 1, we still need to find the jump in amplitude of the derivative at the discontinuities $\hat{f}'(\varphi)$.

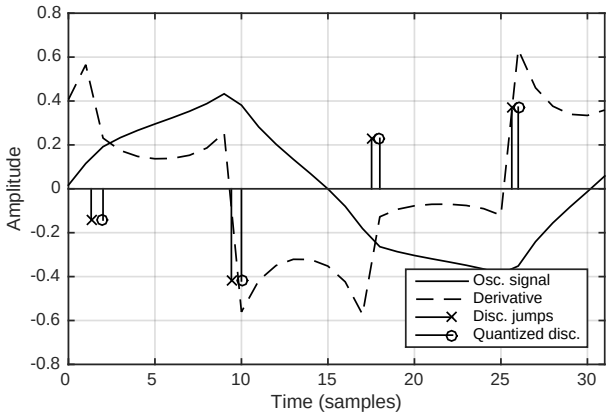

Figure 2: *Signal $f(\varphi)$ of order $n = 3.75$ and pitch $f_0 = 1415$ Hz with its derivative $f'(\varphi)$. The discontinuities $\hat{f}'(\varphi)$ are shown at exact and quantized positions.*

The closed form derivative of equation (3), $f'_x(\varphi)$ with $a = \frac{\pi}{n}$ is:

$$\frac{\mathrm{d}f_x(\varphi)}{\mathrm{d}\varphi} = \frac{\mathrm{d}}{\mathrm{d}\varphi}\frac{\cos(\varphi)\cos(a)}{\cos\left[\mathrm{mod}\left(\varphi, 2a\right) - a\right]}\ , \tag{6}$$

Treating $\varphi_m = mod(\varphi, 2a)$ as a special case of φ, which needs to be differentiated but marked, yields:

$$f'_x(\varphi) = \cos(a)\frac{\cos(\varphi)\sin(\varphi_m - a) - \sin(\varphi)\cos(\varphi_m - a)}{\cos(\varphi_m - a)^2} \tag{7}$$
$$f'_y(\varphi) = \cos(a)\frac{\cos(\varphi)\cos(\varphi_m - a) - \sin(\varphi)\sin(\varphi_m - a)}{\cos(\varphi_m - a)^2} \tag{8}$$

3.3. Efficient implementation

We are only interested in the change in amplitude of the derivative at the discontinuities $\hat{f}'$, which happens when $\varphi_m \in [0...2a)$ wraps around. Looking from both sides ($\varphi_{m\downarrow} = 0$ and $\varphi_{m\uparrow} = 2a$) yields:

$$\lim_{\varphi_m \downarrow 0} \hat{f}_x{}'(\varphi) = \quad \hat{f}'_\downarrow(\varphi) = \frac{-\sin(\varphi)\cos(a) + \sin(a)\cos(\varphi)}{\cos(a)} \tag{9}$$
$$\lim_{\varphi_m \uparrow 2a} \hat{f}_x{}'(\varphi) = \quad \hat{f}'_\uparrow(\varphi) = \frac{-\sin(\varphi)\cos(a) - \sin(a)\cos(\varphi)}{\cos(a)} \tag{10}$$

This leaves us with a simple expression for the change in amplitude at discontinuities:

$$\hat{f}'(\varphi) = \hat{f}'_\downarrow(\varphi) - \hat{f}'_\uparrow(\varphi) = -2\tan(a)\cos(\varphi) \tag{11}$$

Using Equation (11), we can now correctly scale the residuum of Table 1. Figure 3 shows the original function and its anti-aliased version as well as their difference, with is zero everywhere except the 4 samples surrounding a discontinuity.

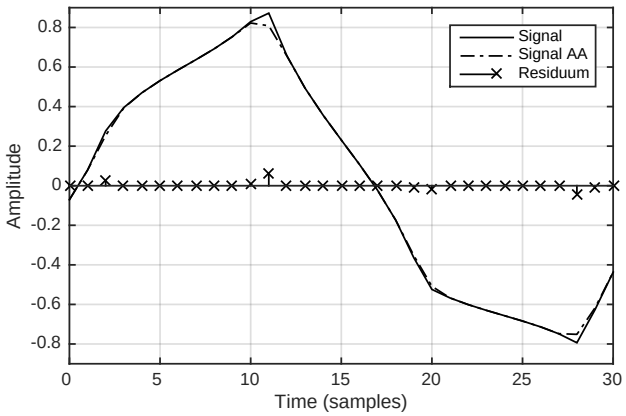

Figure 3: *Original and anti-aliased versions of the signal $f(\varphi)$ of order $n = 3.75$ and pitch $f_0 = 1350$ Hz.*

4. RESULTS

In the following Section, the presented method is compared to traditional oversampling (2x and 4x) in terms of Signal-to-Noise Ratio (SNR) and computational load.

4.1. Signal-to-Noise Ratio

Sharp discontinuities exhibit unbounded frequency requirements, which results in foldback at $f_{\text{NY}} = f_s/2$ and effectively raises the noise floor of the oscillator. Therefore, the Signal-to-Noise Ratio (SNR), which denotes the ratio between the energy in the fundamental + harmonics and that of the rest of the spectrum is a good metric for measuring and comparing the performance of different anti-aliasing approaches.

Firstly, the harmonic overtones $f_{\text{H,k}}$, which depend on order n and the fundamental pitch f_0, need to be determined. For the continuous order polygonal oscillator, the frequencies of the first K harmonics $f_{\text{H, k}}$ can be found to be:

$$f_{\text{H,k}}(f_0, n) = f_0 \left(2 \left\lfloor \frac{k}{2} \right\rfloor + 1 + (n-2)(1 + \left\lfloor \frac{k-1}{2} \right\rfloor) \right) , \tag{12}$$

where $\lfloor \cdot \rfloor$ denotes the flooring function, n is the order, f_0 the fundamental frequency and $k \in [1...K]$.

The energy of the fundamental and harmonics is extracted directly from the Fourier spectrum, the noise energy is simply the difference of the full and the signal energy:

$$\text{SNR} = \frac{E_{\text{sig}}}{E_{\text{noise}}} = \frac{\sum |f_0 + f_H|^2}{\sum |f_\forall|^2 - \sum |f_0 + f_H|^2} \tag{13}$$

The SNR can then be calculated for both the original signal and various anti-aliased versions. While the measured SNR depends on order n as well as the fundamental frequency f_0, large improvements of the SNR on the magnitude of 20 dB compared to the original signal were found consistently, as shown in Table 2. It can be seen that the measured improvements of the employed method falls between $2\times$ and $4\times$ oversampling, which was implemented using a 64 / 128 ($2\times/4\times$ oversampling) order FIR lowpass filter and Matlab's Polyphase FIR decimator as implemented in the `dsp.FIRDecimator` object.

		SNR (dB)			
f_0	n	original	2x OX	4x OX	BLAMP
400 Hz	2.53	57.2	72.5	82	78.7
751 Hz	4.42	66.7	82.6	94	87.8
1350 Hz	3.75	59.4	74	83.6	80.3

Table 2: SNR at different pitches f_0 and orders n of the original signal, 2x oversampling, 4x oversampling and our BLAMP implementation.

Figure 4 shows the Fourier spectra of the original (top) and three anti-aliased versions: 2x oversampling (second), 4x oversampling (third) and closed form BLAMPS (bottom), with the overtones of the fundamental marked in each. The chosen settings correspond to Table 2 and are $n = 2.53$, $f_0 = 400$ Hz in Fig. 4a) and $n = 3.75$, $f_0 = 1350$ Hz in Fig. 4b. Although the three anti-aliased versions exhibit slightly different characteristics, the lowered noise floor can be seen clearly in each. In both oversampling cases, a considerate drop in harmonics close to $f_s/2$ can be observed due to the low-pass filtering before decimation, as well as a uniformly suppressed noise floor. On the other hand, the BLAMP implementation exhibits only a small drop in high-frequency harmonics and has a continuously decreasing noise floor.

The stronger aliasing at higher frequencies, although less audible, lowers the overall SNR measurement of the BLAMP approach which uniformly weights all anti-aliasing noise. This is an advantage that is not easy to measure but arguably of large importance - BLAMP suppresses the potentially more disturbing anti-aliasing artifacts (below 10 kHz) stronger compared to other approaches.

4.2. Performance

As shown above, relatively large improvements in SNR can be achieved quite efficiently by precisely analysing the oscillator function at hand. The validity of the derivation is limited to the points at the discontinuities but for a given order, only a single trigonometric function has to be evaluated.

Compared to traditional oversampling, the presented approach falls in between 2x and 4x oversampling in terms of SNR improvement, as shown in Table 2. However, oversampling involves three computationally expensive steps (upsampling - lowpass - downsampling), which on a current machine come with an averaged 25x performance hit when comparing execution times in Matlab.

5. CONCLUSIONS

It was shown that even for non-traditional digital oscillators, elegant and computationally cheap solutions for the polyBLAMP anti-aliasing approach may be found by only considering the necessary points of discontinuity. For an oscillator method that inherently generates high levels of aliasing noise such as the one presented, this can increase the SNR by 20 dB - beating $2\times$ oversampling - at 25x lower computational complexity. The perceptual comparison are even be more favorable, as the polyBLAMP method continuously drives down the noise floor (compared to constant uniform suppression of oversampling methods) which results in lower aliasing artifacts at audible frequencies below 10 kHz.

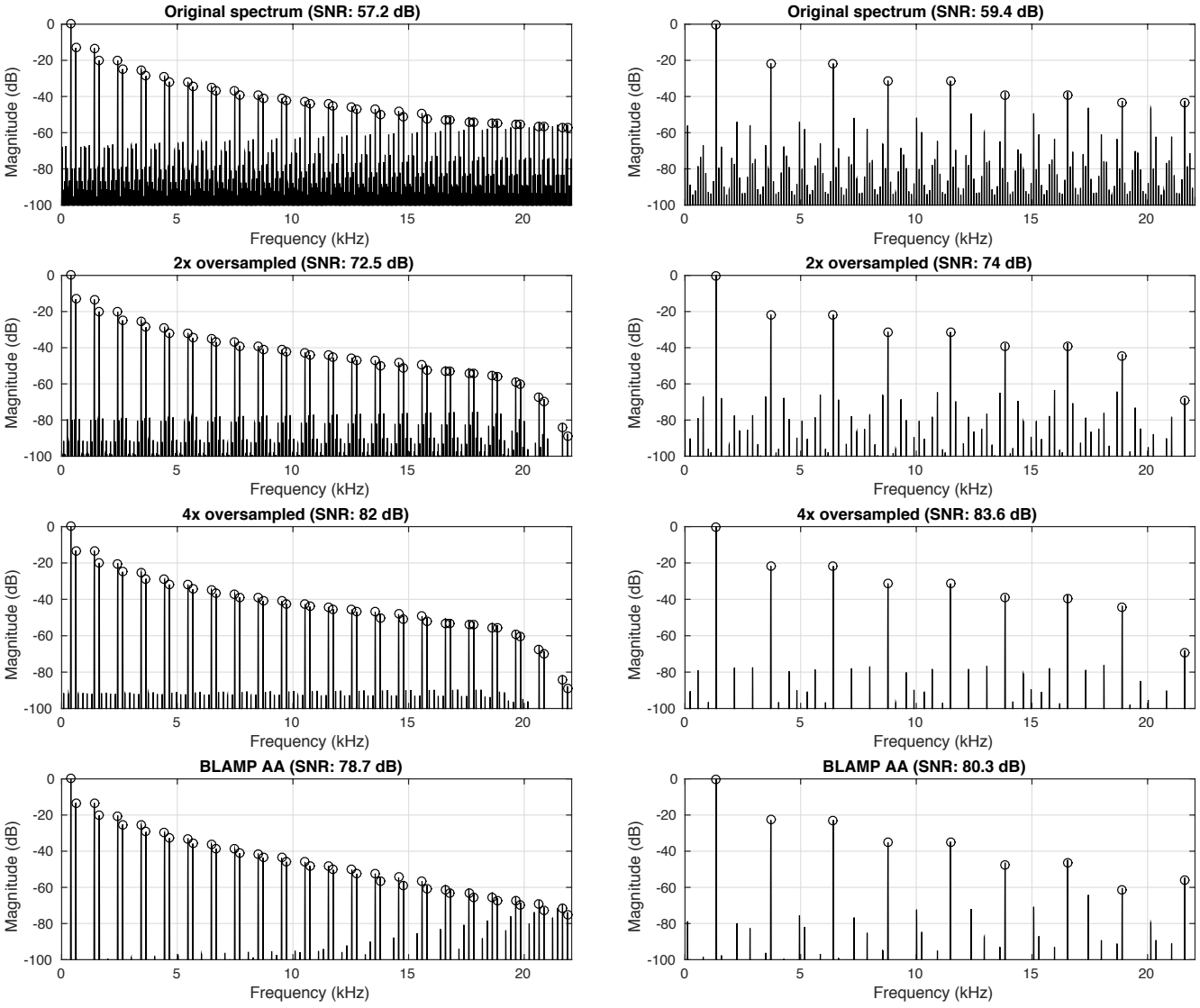

(a) *Order* $n = 2.53$, *fundamental pitch* $f_0 = 400\,Hz$.

(b) *Order* $n = 3.75$, *fundamental pitch* $f_0 = 1350\,Hz$.

Figure 4: *Magnitude spectra of the polygonal oscillator at different settings and different anti-aliasing strategies. Original (top), 2x oversampled (second), 4x oversampled (third) and BLAMP anti-aliased (bottom). Sampling frequency* $f_s = 44.1\,kHz$, *fundamental and harmonics used for SNR computation marked with* $\circ$.

6. REFERENCES

[1] C. Hohnerlein, M. Rest, and J. O. Smith III, "Continuous order polygonal waveform synthesis," in *Proceedings of the International Computer Music Conference*, Utrecht, Netherlands, Sept. 12-16, 2016, pp. 533–536.

[2] Tim Stilson and Julius Smith, "Alias-free digital synthesis of classic analog waveforms," in *Proceedings of the International Computer Music Conference*, Hong Kong, 1996, pp. 332–335.

[3] E. Brandt, "Hard sync without aliasing," in *Proc. Int. Computer Music Conf.*, Havana, Cuba, Sept. 2001, pp. 365–368.

[4] V. Välimäki and A. Huovilainen, "Oscillator and filter algorithms for virtual analog synthesis," *Computer Music J.*, vol. 30, no. 2, pp. 19–31, 2006.

[5] V. Välimäki and A. Huovilainen, "Antialiasing oscillators in subtractive synthesis," *IEEE Signal Process. Mag.*, vol. 24, no. 2, pp. 116–125, 2007.

[6] J. Pekonen, J. Nam, J. O. Smith, J. Abel, and V. Välimäki, "On minimizing the look-up table size in quasi-bandlimited classical waveform oscillators," in *Proc. Int. Conf. Digital Audio Effects (DAFx-10)*, Graz, Austria, Sept. 2010, pp. 419–422.

[7] Vesa Välimäki, Jussi Pekonen, and Juhan Nam, "Perceptually informed synthesis of bandlimited classical waveforms using integrated polynomial interpolation," *The Journal of the Acoustical Society of America*, vol. 131, no. 1, pp. 974–986, 2012.

[8] V. Välimäki, "Discrete-time synthesis of the sawtooth waveform with reduced aliasing," *IEEE Signal Process. Lett.*, vol. 12, no. 3, pp. 214–217, Mar. 2005.

[9] V. Välimäki, J. Nam, J. O. Smith, and J. S. Abel, "Alias-suppressed oscillators based on differentiated polynomial waveforms," *IEEE Trans. Audio Speech Lang. Process.*, vol. 18, no. 4, pp. 786–798, May 2010.

[10] A. Franck and V. Välimäki, "Higher-order integrated wavetable and sampling synthesis," *J. Audio Eng. Soc.*, vol. 61, no. 9, pp. 624–636, Sept. 2013.

[11] A. Franck and V. Välimäki, "An ideal integrator for higher-order integrated wavetable synthesis," in *Proc. IEEE Int. Conf. Acoust. Speech Signal Process. (ICASSP-13)*, Vancouver, BC, Canada, May 2013, pp. 41–45.

[12] J. Kleimola and V. Välimäki, "Reducing aliasing from synthetic audio signals using polynomial transition regions," *IEEE Signal Process. Lett.*, vol. 19, no. 2, pp. 67–70, Feb. 2012.

[13] D. Ambrits and B. Bank, "Improved polynomial transition regions algorithm for alias-suppressed signal synthesis," in *Proc. 10th Sound and Music Computing Conf. (SMC2013)*, Stockholm, Sweden, Aug. 2013, pp. 561–568.

[14] J. D. Parker, V. Zavalishin, and E. Le Bivic, "Reducing the aliasing of nonlinear waveshaping using continuous-time convolution," in *Proc. Int. Conf. Digital Audio Effects (DAFx-16)*, Brno, Czech Republic, Sept. 2016, pp. 137–144.

[15] S. Bilbao, F. Esqueda, J. Parker, and V. Valimaki, "Antiderivative antialiasing for memoryless nonlinearities," *IEEE Signal Processing Letters*, vol. PP, no. 99, pp. 1–1, 2017.

[16] F. Esqueda, V. Välimäki, and S. Bilbao, "Aliasing reduction in soft-clipping algorithms," in *Proc. European Signal Processing Conf. (EUSIPCO 2015)*, Nice, France, Aug. 2015, pp. 2059–2063.

[17] F. Esqueda, S. Bilbao, and V. Välimäki, "Aliasing reduction in clipped signals," *IEEE Trans. Signal Process.*, vol. 60, no. 20, pp. 5255–5267, Oct. 2016.

[18] F. Esqueda, V. Välimäki, and S. Bilbao, "Rounding corners with BLAMP," in *Proc. Int. Conf. Digital Audio Effects (DAFx-16)*, Brno, Czech Republic, Sept. 2016, pp. 121–128.